7-1-2007

Radial velocities of six OB stars

T. S. Boyajian
Georgia State University

D. R. Gies
Georgia State University

E. K. Baines
Georgia State University

P. Barai
Georgia State University

E. D. Grundstrom
Georgia State University

See next page for additional authors

Recommended Citation

Boyajian, T., Gies, D., Baines, E., Barai, P., Grundstrom, E., Mcswain, M., Parks, J., Riddle, R., Ryle, W., & Wingert, D. (2007). Radial velocities of six OB stars. *Publications of the Astronomical Society of the Pacific, 119* (857), 742-746. https://doi.org/10.1086/520707

Radial Velocities of Six OB Stars

T. S. Boyajian[1], D. R. Gies[1],
E. K. Baines, P. Barai[2], E. D. Grundstrom[1], M. V. McSwain[1,3,4],
J. R. Parks, R. L. Riddle[1,5], W. T. Ryle, and D. W. Wingert[1]

Center for High Angular Resolution Astronomy and
Department of Physics and Astronomy,
Georgia State University, P.O. Box 4106, Atlanta, GA 30302-4106;
tabetha@chara.gsu.edu, gies@chara.gsu.edu, baines@chara.gsu.edu, pabar56@phy.ulaval.ca,
erika@chara.gsu.edu, mcswain@astro.yale.edu, parksj@physics.emory.edu,
riddle@astro.caltech.edu, ryle@chara.gsu.edu, wingert@chara.gsu.edu

ABSTRACT

We present new results from a radial velocity study of six bright OB stars with little or no prior measurements. One of these, HD 45314, may be a long-period binary, but the velocity variations of this Be star may be related to changes in its circumstellar disk. Significant velocity variations were also found for HD 60848 (possibly related to nonradial pulsations) and HD 61827 (related to wind variations). The other three targets, HD 46150, HD 54879, and HD 206183, are constant velocity objects, but we note that HD 54879 has Hα emission that may originate from a binary companion. We illustrate the average red spectrum of each target.

Subject headings: Binaries: spectroscopic — stars: early-type — stars: emission-line, Be — stars: individual (HD 45314, HD 46150, HD 54879, HD 60848, HD 61827, HD 206183)

---

[1]Visiting Astronomer, Kitt Peak National Observatory, National Optical Astronomy Observatory, operated by the Association of Universities for Research in Astronomy, Inc., under contract with the National Science Foundation.

[2]Current Address: Departement de physique, de genie physique et d'optique, Universite Laval, Pavillon Alexandre-Vachon, Quebec, QC G1K 7P4, Canada

[3]Current Address: Astronomy Department, Yale University, New Haven, CT 06520-8101

[4]NSF Astronomy and Astrophysics Postdoctoral Fellow

[5]Current Address: Thirty Meter Telescope, 2632 E. Washington Blvd., Pasadena, CA 91107

1. Introduction

Radial velocity measurements exist for many of the bright OB stars because of their usefulness for binary mass determination and cluster dynamics. However, in a survey of the multiplicity of bright O-stars, Mason et al. (1998) listed some 17 of 227 stars without sufficient radial velocity data to determine whether or not the stars were members of spectroscopic binaries. We observed six of these targets with unknown spectroscopic duplicity in two extended observing runs of high dispersion and high S/N spectroscopy at the Kitt Peak National Observatory (KPNO) coudé feed telescope in 2000. We have already reported on discoveries made during these runs of new single-lined spectroscopic binaries (HD 14633, HD 15137; Boyajian et al. 2005) and double-lined spectroscopic binaries (HD 37366, HD 54662; Boyajian et al. 2007). Here we present our results on the six of the stars with mainly "unknown" spectroscopic binary status from the list of Mason et al. (1998). We describe the observations, measurements, and analysis in §2 and then discuss the individual targets in detail in §3. Our results are summarized in Table 2 of §2.

2. Observations and Radial Velocities

Red spectra were collected with the KPNO 0.9 m coudé feed telescope during two observing runs in 2000 October and 2000 December. The spectra were made using the long collimator, grating B (in second order with order sorting filter OG 550), camera 5, and the F3KB CCD, a Ford Aerospace 3072×1024 device. The setup yielded a resolving power of $R = \lambda/\delta\lambda \approx 9500$, with a spectral coverage of $6440 - 7105$ Å. The exposure times were less than 30 minutes yielding a $S/N \approx 200$ per pixel. We obtained between 22 and 62 spectra of each star.

The spectra were extracted and calibrated using standard routines in *IRAF*[6], and then each continuum rectified spectrum was transformed onto a uniform heliocentric wavelength grid for analysis. We removed atmospheric lines by creating a library of spectra from each run of the rapidly rotating A-star ζ Aql, removing the broad stellar features from these, and then dividing each target spectrum by the modified atmospheric spectrum that most closely matched the target spectrum in a selected region dominated by atmospheric absorptions.

We measured radial velocities in two ways. For targets with absorption lines, we formed

[6]IRAF is distributed by the National Optical Astronomy Observatory, which is operated by the Association of Universities for Research in Astronomy, Inc., under cooperative agreement with the National Science Foundation.

a cross-correlation function (ccf) between a given spectrum and a single reference spectrum of the star (usually the first observation). These relative velocities were then transformed to an absolute velocity scale by adding a mean velocity measured by parabolic fits to the lower halves of the absorption lines in the reference spectrum. Two of the targets have spectra dominated by emission lines and in these cases we measured bisector velocities for the extreme line wings using the method of Shafter, Szkody, & Thorstensen (1986). All these velocities are shown in Table 1[7], which lists the star name, heliocentric Julian date of mid-exposure, radial velocity, and the line-to-line standard deviation σ (where multiple lines were measured). In §3, we give a more detailed description of the radial velocity analysis performed on the individual stars.

We checked for evidence of temporal variations in the velocity data by comparing the external scatter between observations E (equal to the standard deviation of the individual velocities in Table 1) with an estimate of the internal error I. The internal error is the average of the line-to-line standard deviation σ for all but the cases of HD 45314 and HD 60848 where only one spectral feature was measured. For these two cases, we estimated I by the average of $|V_i - V_{i+1}|/\sqrt{2}$ for observations closely spaced in time. We then computed the F-statistic to determine the probability that the observed scatter is due to random noise (Conti, Garmany, & Hutchings 1977a). We assume that the variations are significant if this probability is below 1% (Conti et al. 1977a). The results are summarized in Table 2 that lists the star name, number of observations, the mean velocity, E, I, the derived probability, and a short description of the probable source of the variations if present. Details for each target follow in the next section.

3. Notes on Individual Stars

3.1. HD 45314

The star HD 45314 (O9 pe, Conti 1974; B0 IVe, Negueruela, Steele, & Bernabeu 2004) has a speckle interferometric companion at a separation of 50 mas (corresponding to a period of ≈ 30 y; Mason et al. 1998). The average red spectrum illustrated in Figure 1 shows that Hα and He I$\lambda\lambda$6678, 7065 are double-peaked emission lines. This suggests that the emission forms in a disk and that the line wings form in the gas closest to the star. Thus, we can use measurements of the Hα wings as a proxy for the motion of the underlying star. We measured radial velocities using the wing bisector method of Shafter et al. (1986).

[7]Available in full in the electronic version of the paper.

Our results indicate that there was a significant change in velocity from -32.0 ± 0.9 km s^{-1} to -21.6 ± 1.9 km s^{-1} between the runs. This may indicate that the Be star is a spectroscopic binary with a period of months. However, the emission profiles changed in shape between the runs (see Fig. 2 for the Hα averages from each run), so it is also possible that the changes in bisector velocity result from physical changes in the gas distribution in the disk rather than orbital motion. We recommend a program of blue spectroscopy of this star to distinguish between the binary and disk variation explanations.

3.2. HD 46150

The spectroscopic binary status of HD 46150 (O5 V((f)); Underhill & Gilroy 1990) remains inconclusive even though it has a history of radial velocity measurements spanning eight decades (Plaskett 1924; Abt 1970; Conti, Leep, & Lorre 1977b; Garmany, Conti, & Massey 1980; Liu, Janes, & Bania 1989, 1991; Underhill & Gilroy 1990; Fullerton 1990; Stickland & Lloyd 2001). The measured radial velocities fall in the range of $V_r = 14-51$ km s^{-1}. Stickland & Lloyd (2001) suggest that this range is significantly larger than expected for diverse measurements of a single star. The most extensive analysis of this star by Garmany et al. (1980) covered four observing seasons, with a mean $V_r = 39$ km s^{-1} and a range of 26 km s^{-1}. They conclude that the scatter results from atmospheric rather than orbital variations (see also Underhill & Gilroy 1990).

The mean red spectrum in Figure 3 shows a strong He II spectrum associated with a very early-type star. We measured ccf velocities of the Hα, He I $\lambda\lambda 6678, 7065$, and He II $\lambda\lambda 6683, 6890$ features. The error in the mean velocity from closely spaced pairs is $I = 1.3$ km s^{-1} while the standard deviation among the mean velocities is $E = 3.8$ km s^{-1}. A standard F-test (Conti, Garmany, & Hutchings 1977a) indicates that a temporal variation this large is expected by random variations with a probability of 0.6%, i.e., the observed variation is probably significant. However, most of the variance comes from the first run where there appear to be relatively large night-to-night variations that are absent in the second run. This may indicate that the observational errors were larger in the first run compared to our estimate of I from the scatter in measurements from the second run (also consistent with the larger line-to-line scatter in σ for the first run). Thus, the velocity variations are probably not significant and are consistent with constant radial velocity over the interval of our observations.

3.3. HD 54879

The target HD 54879 (B3 V, Neubauer 1943; O9.5 V, Morgan, Code, & Whitford 1955; B0 V, Claria 1974) has only a few spectroscopic measurements over the past century. The mean spectrum shown in Figure 4 indicates that it has Hα emission and is thus a Be star, which has historically never been observed in emission until now. We made ccf velocity measurements using the lines He I $\lambda\lambda 6678, 7065$, C II $\lambda\lambda 6578, 6583$, and Si IV $\lambda\lambda 6667, 6701$.

Our V_r measurements show no evidence of Doppler shifts in the absorption lines over both short and long timescales. The external error $E = 1.4$ km s^{-1} is somewhat larger than the internal error $I = 0.6$ km s^{-1}. The F-test indicates that a scatter between observations of this size is expected with a probability of 3.1%, so this star is radial velocity constant over the duration of the runs. The only other radial velocity measurement on record from Neubauer (1943), $V_r = 15.6 \pm 1.4$ km s^{-1}, is smaller than our mean of $V_r = 35.4 \pm 1.4$ km s^{-1}. We caution that this discrepancy may be caused by measuring different lines in the blue part of the spectrum or by long term changes in the spectrum.

The mean spectrum has very narrow lines of He I, C II, N II, O II, and Si IV. These apparently sharp absorption lines are unexpected in Be stars that are normally rapid rotators with broad lines. One possibility is that HD 54879 is a rare Be star that is seen almost pole-on, so that the rotation is tangential to the line of sight and the lines do not suffer rotational broadening. Another possibility is that HD 54879 is a Be shell star in which the narrow absorptions form in a circumstellar disk that is projected against the star. The star might have a strong magnetic field that controls the gas outflow and that has spun down the star. Finally, the spectrum may be that of a long period binary consisting of a bright, narrow-lined B-star and a fainter Be star (although no companion was found in the speckle survey by Mason et al. 1998). This explanation is supported by the fact that the Hα emission does vary in strength and shape on short and long timescales in our observations while the absorption lines are constant.

3.4. HD 60848

The star HD 60848 is another Be-type object (O9.5 IVe, Negueruela et al. 2004) that may be a runaway star because of its position well out of the Galactic plane (de Wit et al. 2005). It was recently observed with moderate dispersion blue spectra by McSwain et al. (2007) who found no evidence of velocity variability. We observed this star only during the second run, but with a higher sampling rate (as frequent as fifteen minute intervals during some nights). The mean red spectrum (Fig. 5) shows that Hα and He I $\lambda\lambda 6678, 7065$ all

display double-peaked emission.

We measured relative radial velocities by determining ccf offsets from the first spectrum for the He I λ6678 region, and then these were placed on an absolute scale by finding the bisector velocity of the profile in the first spectrum using the method from Shafter et al. (1986). The external error of $E = 3.2$ km s^{-1} is larger than the internal error of $I = 1.0$ km s^{-1}, and the F-test indicates that this scatter has a probability of 0.3% for an origin in random variations. Furthermore, there is clear evidence of systematic trends within some nights. We used the CLEAN algorithm from Roberts, Lehár, & Dreher (1987) to find evidence of two periodic signals with periods of 3.51 ± 0.03 and 3.74 ± 0.03 hours (both with peak power far above the 1% false alarm probability defined by Scargle 1982). These periods are much too small to be related to binary motion. They may be due to changes in disk density or illumination caused by nonradial pulsations in the underlying star (Rivinius, Baade, & Štefl 2003).

3.5. HD 61827

The star HD 61827 (O8 − 9 Ib, Houk 1982; B3 Iab, Garrison, Hiltner, & Schild 1977; B3 Ia, Turner 1977) is a luminous object in an association surrounding the cluster NGC 2439 (Turner 1977). We found no evidence of a prior radial velocity measurement in the literature. The star's red spectrum (Fig. 6) shows Hα in emission as is often the case for B-supergiants. The lack of He II λ6683 and the relative strength of C II $\lambda\lambda 6578, 6583$ support the later subtype adopted by Garrison et al. (1977) and Turner (1977). We used the C II $\lambda\lambda 6578, 6583$ and He I $\lambda\lambda 6678, 7065$ absorption lines in the ccf to determine radial velocities for this star. The ratio of the external to the internal error indicates that the star is a velocity variable.

Our spectra show dynamic Hα emission changes with variable red and blue peaks appearing to vary on a timescale of 5 – 10 d. We suspect that these variations are related to structures in the stellar wind that are modulated by rotation and temporal changes in the outflow. These emission variations in Hα appear to affect the velocities measured for the absorption lines of C II and He I through subtle effects of emission filling that are not apparent to the eye. For example, during the first run we observed the emergence of a strong redshifted Hα peak during the time when the absorption velocities attained their minimum value, and the appearance of a strongly blueshifted Hα peak occurred at the time when the absorption velocities reached a maximum. This correlation indicates that the absorption lines we measured (C II and He I) are probably also partially filled in by weak emission that shifts the line center away from the location of the emission. Thus, we suggest that the apparent velocity variations in HD 61827 are due to the effects of variations in the star's

wind.

3.6. HD 206183

HD 206183 (O9.5 V, Daflon et al. 2003) resides in the Tr 37 cluster in the Cep OB2 association. Mason et al. (1998) list two visual companions, but assign the star to the "unknown" status as a spectroscopic binary since only one other velocity measurement exists (Sanford & Merrill 1938). The average red spectrum (Fig. 7) shows that the lines are narrow ($V \sin i = 19.2 \pm 1.9$ km s^{-1}; Daflon et al. 2003). We measured ccf radial velocities for HD 206183 using Hα and He I $\lambda\lambda 6678, 7065$. The mean velocities show no evidence for velocity variability over the two runs.

We thank Daryl Willmarth and the staff of KPNO for their assistance in making these observations possible. This work was supported by the National Science Foundation under grants AST-0205297, AST-0506573, and AST-0606861. Institutional support has been provided from the GSU College of Arts and Sciences and from the Research Program Enhancement fund of the Board of Regents of the University System of Georgia, administered through the GSU Office of the Vice President for Research.

REFERENCES

Abt, H. A. 1970, ApJS, 19, 387

Boyajian, T. S. et al. 2005, ApJ, 621, 978

——. 2007, ApJ, 665, in press

Claria, J. J. 1974, A&A, 37, 229

Conti, P. S. 1974, ApJ, 187, 539

Conti, P. S., Garmany, C. D., & Hutchings, J. B. 1977a, ApJ, 215, 561

Conti, P. S., Leep, E. M., & Lorre, J. J. 1977b, ApJ, 214, 759

Daflon, S., Cunha, K., Smith, V. V., & Butler, K. 2003, A&A, 399, 525

de Wit, W. J., Testi, L., Palla, F., & Zinnecker, H. 2005, A&A, 437, 247

Fullerton, A. W. 1990, Ph.D. thesis, Univ. Toronto

Garmany, C. D., Conti, P. S., & Massey, P. 1980, ApJ, 242, 1063

Garrison, R. F., Hiltner, W. A., & Schild, R. E. 1977, ApJS, 35, 111

Houk, N. 1982, Catalogue of two-dimensional spectral types for the HD stars, Vol. 3 (Michigan Spectral Survey, Ann Arbor, Dept. Astron., Univ. Michigan)

Liu, T., Janes, K. A., & Bania, T. M. 1989, AJ, 98, 626

——. 1991, AJ, 102, 1103

Mason, B. D., Gies, D. R., Hartkopf, W. I., Bagnuolo, Jr., W. G., ten Brummelaar, T., & McAlister, H. A. 1998, AJ, 115, 821

McSwain, M. V., Boyajian, T. S., Grundstrom, E. D., & Gies, D. R. 2007, ApJ, 655, 473

Morgan, W. W., Code, A. D., & Whitford, A. E. 1955, ApJS, 2, 41

Negueruela, I., Steele, I. A., & Bernabeu, G. 2004, Astronomische Nachrichten, 325, 749

Neubauer, F. J. 1943, ApJ, 97, 300

Plaskett, J. S. 1924, Publ. Dom. Astrophys. Obs., 2, 285

Rivinius, T., Baade, D., & Štefl, S. 2003, A&A, 411, 229

Roberts, D. H., Lehár, J., & Dreher, J. W. 1987, AJ, 93, 968

Sanford, R. F., & Merrill, P. W. 1938, ApJ, 87, 517

Scargle, J. D. 1982, ApJ, 263, 835

Shafter, A. W., Szkody, P., & Thorstensen, J. R. 1986, ApJ, 308, 765

Stickland, D. J., & Lloyd, C. 2001, Obs., 121, 1

Turner, D. G. 1977, AJ, 82, 805

Underhill, A. B., & Gilroy, K. K. 1990, ApJ, 364, 626

Table 1. Radial Velocity Measurements

Star Name	Date (HJD−2,450,000)	V_r (km s^{-1})	σ (km s^{-1})
HD 45314	1817.942	−31.3	···
HD 45314	1818.945	−32.2	···
HD 45314	1819.936	−31.2	···
HD 45314	1820.931	−32.0	···
HD 45314	1821.931	−32.2	···
HD 45314	1822.926	−31.9	···
HD 45314	1823.866	−32.0	···
HD 45314	1823.987	−32.5	···
HD 45314	1824.888	−31.4	···
HD 45314	1825.004	−30.6	···
HD 45314	1830.956	−34.2	···
HD 45314	1888.841	−24.2	···
HD 45314	1888.849	−23.2	···
HD 45314	1889.906	−23.8	···
HD 45314	1890.883	−24.1	···
HD 45314	1892.849	−25.7	···
HD 45314	1893.897	−23.5	···
HD 45314	1894.867	−23.2	···
HD 45314	1894.940	−22.7	···
HD 45314	1895.892	−19.7	···
HD 45314	1896.815	−21.1	···
HD 45314	1896.927	−20.3	···
HD 45314	1897.814	−20.2	···
HD 45314	1897.921	−19.5	···
HD 45314	1898.823	−21.2	···
HD 45314	1898.933	−21.4	···
HD 45314	1899.820	−21.5	···
HD 45314	1899.927	−21.4	···
HD 45314	1900.813	−19.4	···
HD 45314	1900.920	−19.0	···

Table 1—Continued

Star Name	Date (HJD−2,450,000)	V_r (km s^{-1})	σ (km s^{-1})
HD 45314	1901.800	−19.7	···
HD 45314	1901.929	−19.6	···
HD 46150	1817.950	34.4	18.4
HD 46150	1818.954	25.5	11.6
HD 46150	1819.945	27.0	10.5
HD 46150	1820.982	27.5	10.7
HD 46150	1821.939	27.6	1.6
HD 46150	1822.933	32.6	10.2
HD 46150	1823.874	32.2	6.8
HD 46150	1824.895	41.2	14.8
HD 46150	1825.010	43.2	14.9
HD 46150	1830.962	39.3	17.0
HD 46150	1889.918	34.4	6.4
HD 46150	1890.892	33.5	6.9
HD 46150	1892.887	34.2	7.4
HD 46150	1893.918	31.9	9.3
HD 46150	1894.875	37.5	5.4
HD 46150	1894.947	35.9	6.2
HD 46150	1895.900	35.3	4.6
HD 46150	1895.962	34.6	11.1
HD 46150	1896.823	35.2	5.5
HD 46150	1896.934	33.7	3.4
HD 46150	1897.821	32.8	8.7
HD 46150	1897.929	34.4	3.0
HD 46150	1898.831	32.7	5.6
HD 46150	1898.941	35.8	5.1
HD 46150	1899.828	34.9	5.5
HD 46150	1899.934	32.8	6.5
HD 46150	1900.821	31.4	5.4
HD 46150	1900.928	35.0	5.5

Table 1—Continued

Star Name	Date (HJD−2,450,000)	V_r (km s^{-1})	σ (km s^{-1})
HD 46150	1901.807	33.3	6.0
HD 46150	1901.936	33.3	15.3
HD 54879	1817.976	35.1	1.3
HD 54879	1818.969	37.4	2.7
HD 54879	1819.971	36.6	2.9
HD 54879	1821.978	33.2	2.4
HD 54879	1822.974	33.1	5.2
HD 54879	1823.964	35.4	1.0
HD 54879	1824.910	39.4	2.7
HD 54879	1889.953	33.4	0.3
HD 54879	1890.931	35.5	2.1
HD 54879	1892.911	33.7	2.1
HD 54879	1894.890	34.0	3.1
HD 54879	1894.964	36.5	0.6
HD 54879	1895.940	34.9	1.6
HD 54879	1896.040	35.7	4.1
HD 54879	1896.889	36.3	3.7
HD 54879	1896.958	36.5	2.3
HD 54879	1897.885	35.7	1.8
HD 54879	1897.949	34.8	1.5
HD 54879	1898.897	35.2	1.7
HD 54879	1898.960	35.4	1.4
HD 54879	1899.891	34.8	2.3
HD 54879	1899.953	34.2	4.1
HD 54879	1900.884	36.4	1.8
HD 54879	1900.947	35.4	2.1
HD 54879	1901.892	36.7	1.8
HD 54879	1901.955	35.7	3.8
HD 60848	1890.035	5.4	···
HD 60848	1890.049	4.7	···

Table 1—Continued

Star Name	Date (HJD−2,450,000)	V_r (km s^{-1})	σ (km s^{-1})
HD 60848	1890.918	9.0	···
HD 60848	1891.985	3.9	···
HD 60848	1891.999	3.0	···
HD 60848	1892.934	5.6	···
HD 60848	1892.952	3.2	···
HD 60848	1892.970	0.2	···
HD 60848	1893.953	7.1	···
HD 60848	1893.978	9.6	···
HD 60848	1893.982	11.1	···
HD 60848	1894.006	8.2	···
HD 60848	1895.997	7.8	···
HD 60848	1896.006	11.5	···
HD 60848	1896.004	11.2	···
HD 60848	1896.013	9.1	···
HD 60848	1896.021	10.6	···
HD 60848	1896.982	0.5	···
HD 60848	1896.990	1.5	···
HD 60848	1897.009	2.1	···
HD 60848	1897.017	6.4	···
HD 60848	1897.026	7.2	···
HD 60848	1897.986	−0.2	···
HD 60848	1897.995	0.5	···
HD 60848	1897.994	2.2	···
HD 60848	1898.002	3.1	···
HD 60848	1898.011	4.8	···
HD 60848	1898.020	4.2	···
HD 60848	1898.099	5.9	···
HD 60848	1898.047	6.1	···
HD 60848	1898.056	7.1	···
HD 60848	1898.983	5.0	···

Table 1—Continued

Star Name	Date (HJD−2,450,000)	V_r (km s^{-1})	σ (km s^{-1})
HD 60848	1898.992	3.9	···
HD 60848	1899.000	2.7	···
HD 60848	1899.019	3.7	···
HD 60848	1899.027	2.0	···
HD 60848	1899.037	3.2	···
HD 60848	1899.046	2.8	···
HD 60848	1899.044	4.1	···
HD 60848	1899.053	4.5	···
HD 60848	1899.987	4.9	···
HD 60848	1899.995	3.4	···
HD 60848	1899.994	3.4	···
HD 60848	1900.003	3.7	···
HD 60848	1900.011	3.0	···
HD 60848	1900.022	2.2	···
HD 60848	1900.030	5.0	···
HD 60848	1900.049	8.1	···
HD 60848	1900.970	11.0	···
HD 60848	1900.988	11.0	···
HD 60848	1900.997	12.8	···
HD 60848	1901.005	10.8	···
HD 60848	1901.004	8.8	···
HD 60848	1901.014	7.5	···
HD 60848	1901.022	5.2	···
HD 60848	1901.031	2.7	···
HD 60848	1901.040	1.4	···
HD 60848	1901.989	4.6	···
HD 60848	1901.997	5.4	···
HD 60848	1902.006	4.6	···
HD 60848	1902.004	6.5	···
HD 60848	1902.013	8.6	···

Table 1—Continued

Star Name	Date (HJD−2,450,000)	V_r (km s^{-1})	σ (km s^{-1})
HD 61827	1817.992	71.8	4.6
HD 61827	1818.983	71.7	1.5
HD 61827	1819.985	67.6	1.2
HD 61827	1821.987	66.8	1.5
HD 61827	1822.985	69.4	1.1
HD 61827	1823.992	75.2	0.9
HD 61827	1824.986	86.2	1.7
HD 61827	1831.002	77.1	1.1
HD 61827	1889.927	60.5	3.8
HD 61827	1890.949	67.2	2.8
HD 61827	1893.930	66.7	0.6
HD 61827	1894.905	68.1	1.2
HD 61827	1895.973	68.9	2.1
HD 61827	1896.899	73.4	0.2
HD 61827	1896.968	72.7	0.9
HD 61827	1897.895	68.4	0.3
HD 61827	1897.962	68.1	0.4
HD 61827	1898.907	67.1	2.1
HD 61827	1898.969	68.3	1.5
HD 61827	1899.901	65.2	1.5
HD 61827	1899.963	64.0	1.3
HD 61827	1900.894	67.8	2.0
HD 61827	1900.956	67.4	2.2
HD 61827	1901.902	78.0	1.8
HD 61827	1901.965	77.6	0.7
HD 206183	1817.670	−9.4	2.6
HD 206183	1818.708	−9.2	1.2
HD 206183	1819.864	−6.9	1.5
HD 206183	1820.703	−7.9	1.6
HD 206183	1821.687	−9.3	1.6

Table 1—Continued

Star Name	Date (HJD−2,450,000)	V_r (km s^{-1})	σ (km s^{-1})
HD 206183	1822.691	−7.7	1.6
HD 206183	1823.682	−8.3	0.9
HD 206183	1823.888	−7.2	1.4
HD 206183	1824.664	−4.4	1.2
HD 206183	1824.834	−4.0	1.5
HD 206183	1830.704	−8.1	1.1
HD 206183	1830.879	−7.0	0.8
HD 206183	1890.603	−8.8	1.5
HD 206183	1893.570	−8.7	1.1
HD 206183	1894.566	−8.5	0.4
HD 206183	1895.601	−7.9	1.0
HD 206183	1896.600	−8.5	0.9
HD 206183	1897.596	−8.9	0.6
HD 206183	1898.606	−8.0	0.8
HD 206183	1899.607	−7.4	0.3
HD 206183	1900.603	−7.2	1.7
HD 206183	1901.587	−7.8	1.0

Table 2. Radial Velocity Summary

Star Name	N	$< V_r >$ (km s^{-1})	E (km s^{-1})	I (km s^{-1})	Prob. (%)	Status
HD 45314	33	−25.1	5.2	0.4	0	Long-period SB or disk var.
HD 46150	30	33.8	3.8	1.3	0.6	Constant
HD 54879	26	35.4	1.4	0.6	3.1	Constant
HD 60848	62	5.5	3.2	1.0	0.3	Short-period var.
HD 61827	25	70.2	5.4	0.5	0	Wind-related var.
HD 206183	22	−7.8	1.4	0.6	3.4	Constant

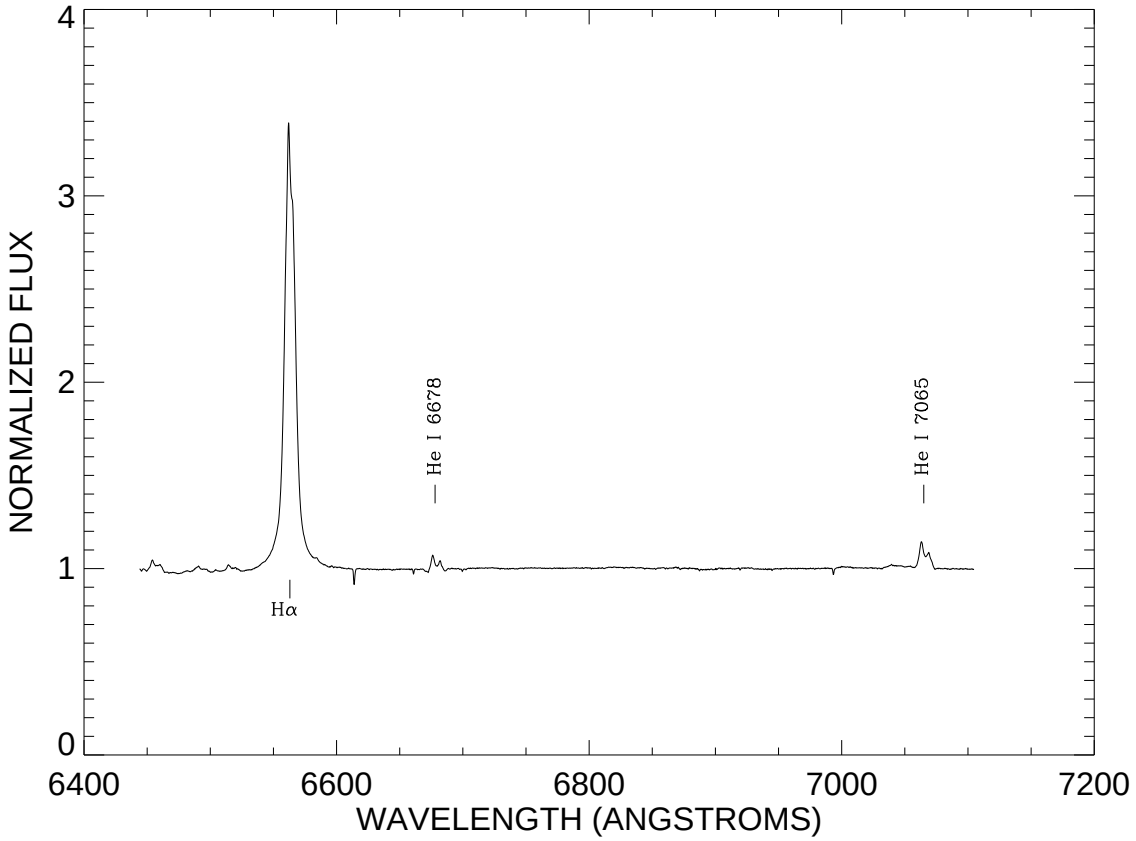

Fig. 1.— Mean red spectrum of HD 45314 in the rest frame. Line identifications are marked by vertical lines.

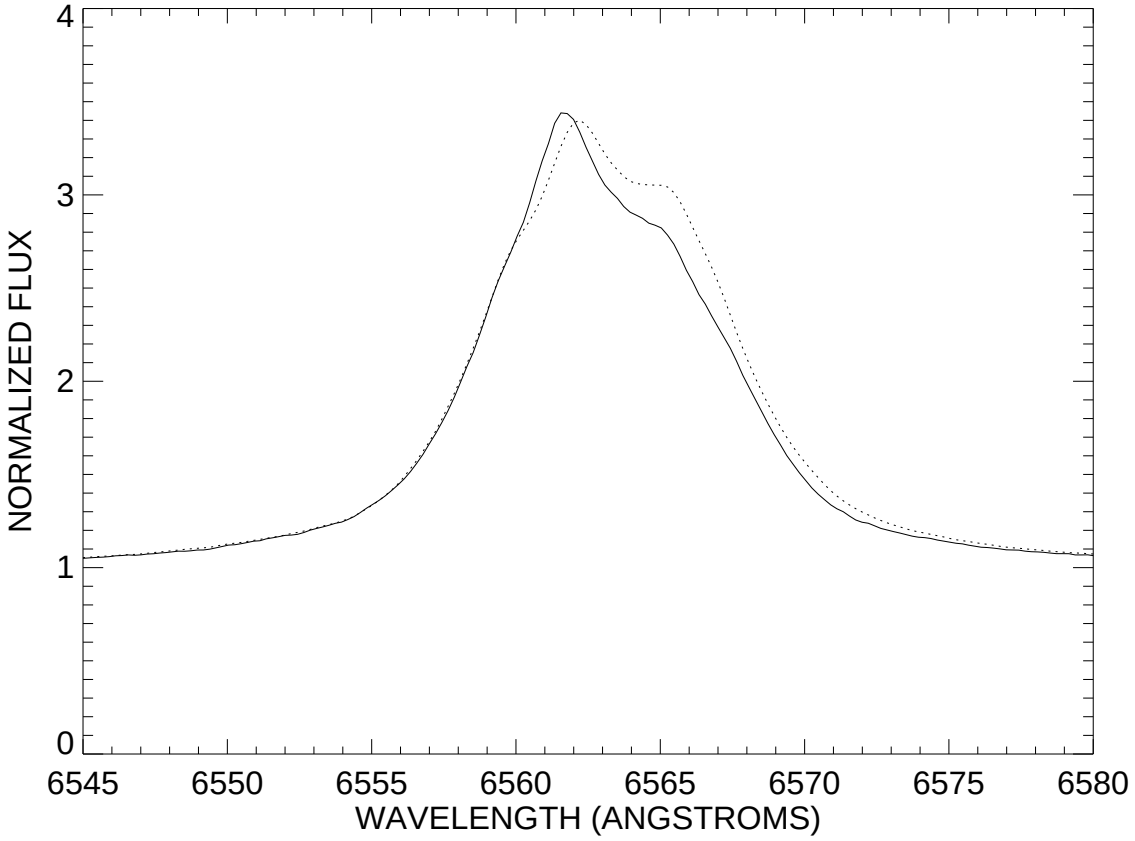

Fig. 2.— HD 45314 mean Hα line profiles observed during the first (*solid line*) and second (*dotted line*) observing runs.

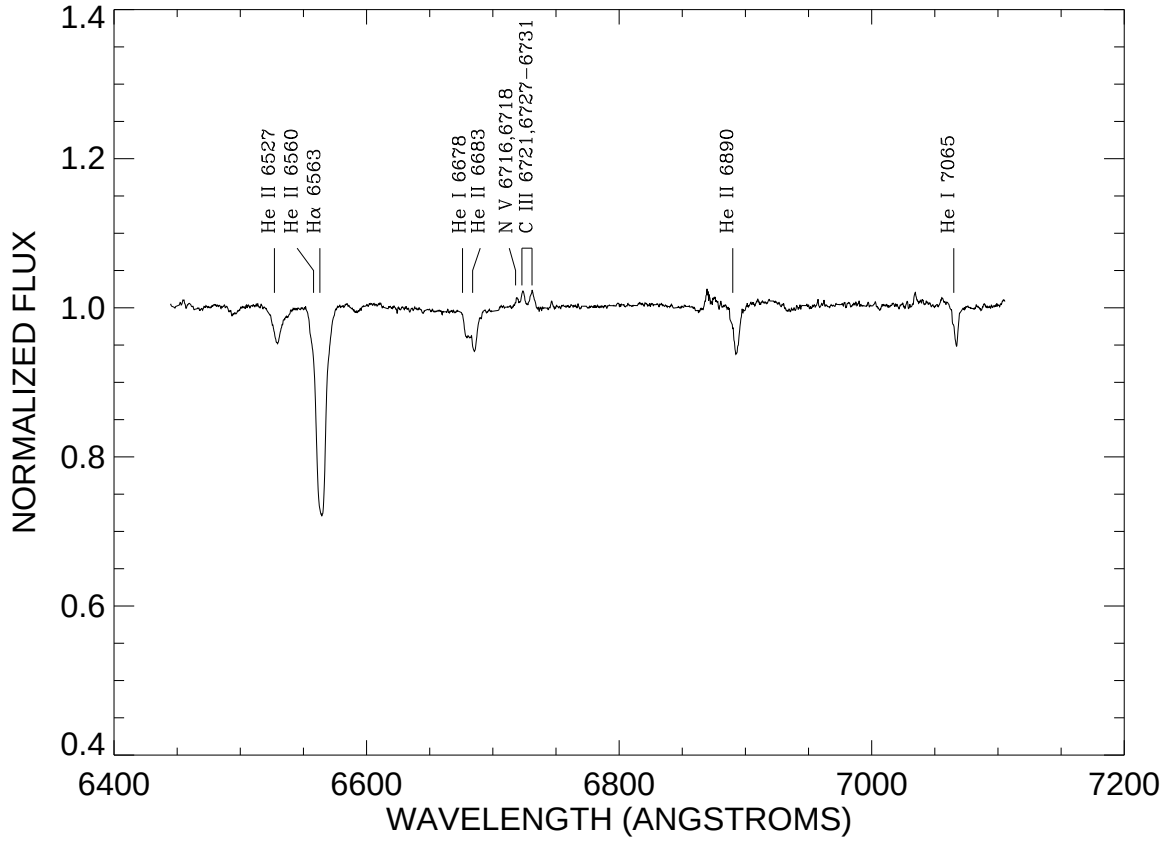

Fig. 3.— Mean spectrum of HD 46150.

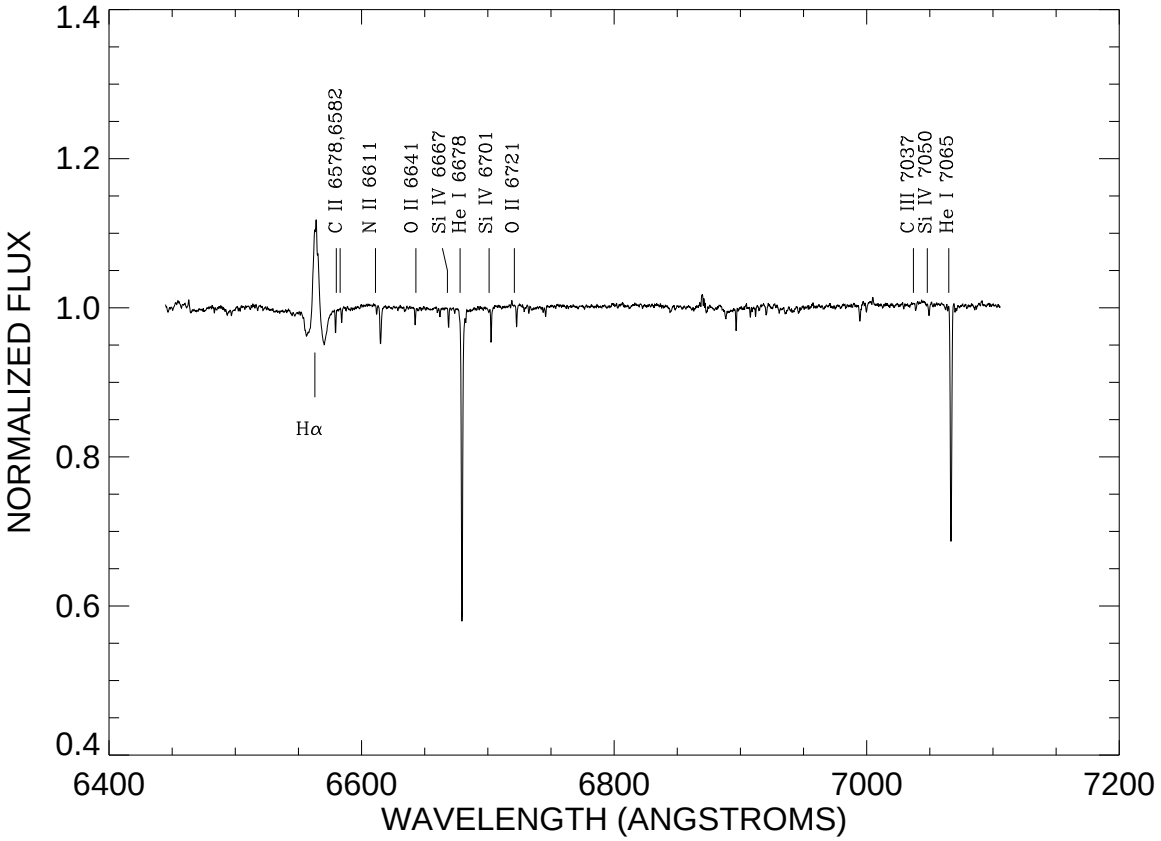

Fig. 4.— Mean spectrum of HD 54879.

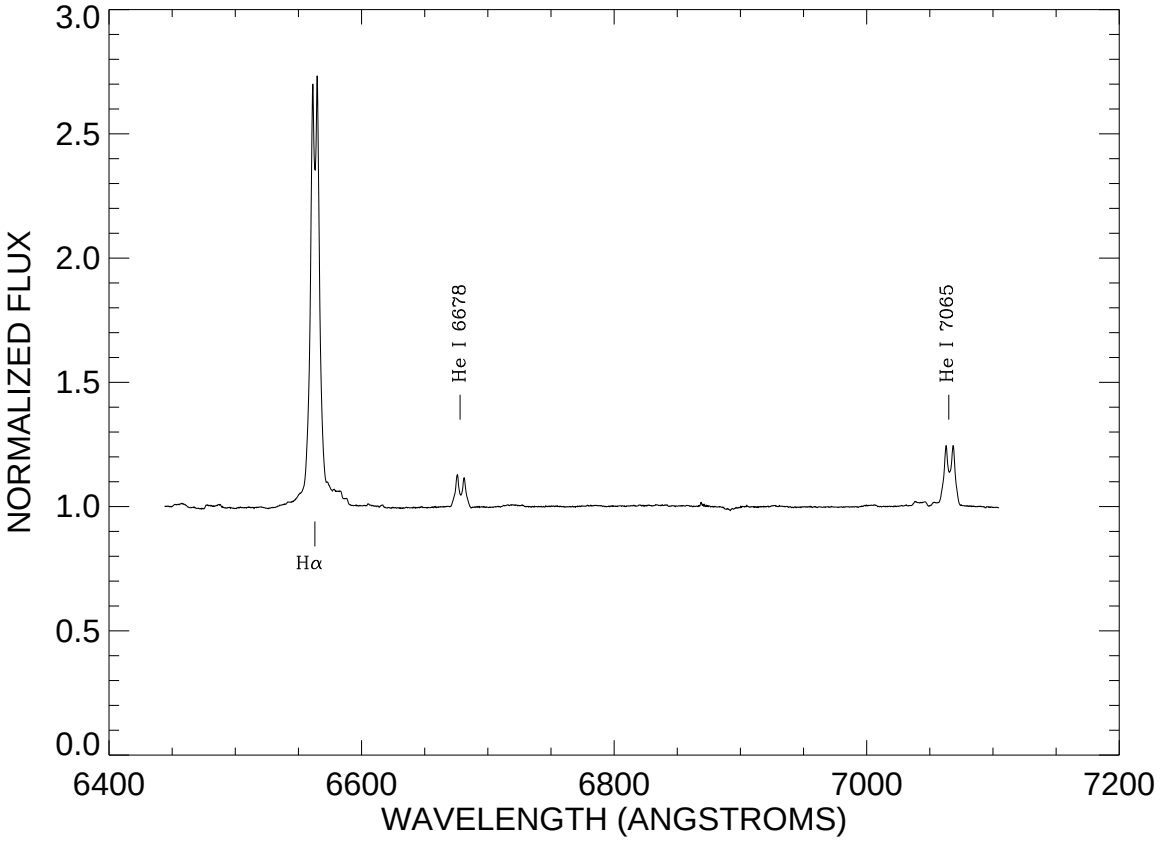

Fig. 5.— Mean spectrum of HD 60848.

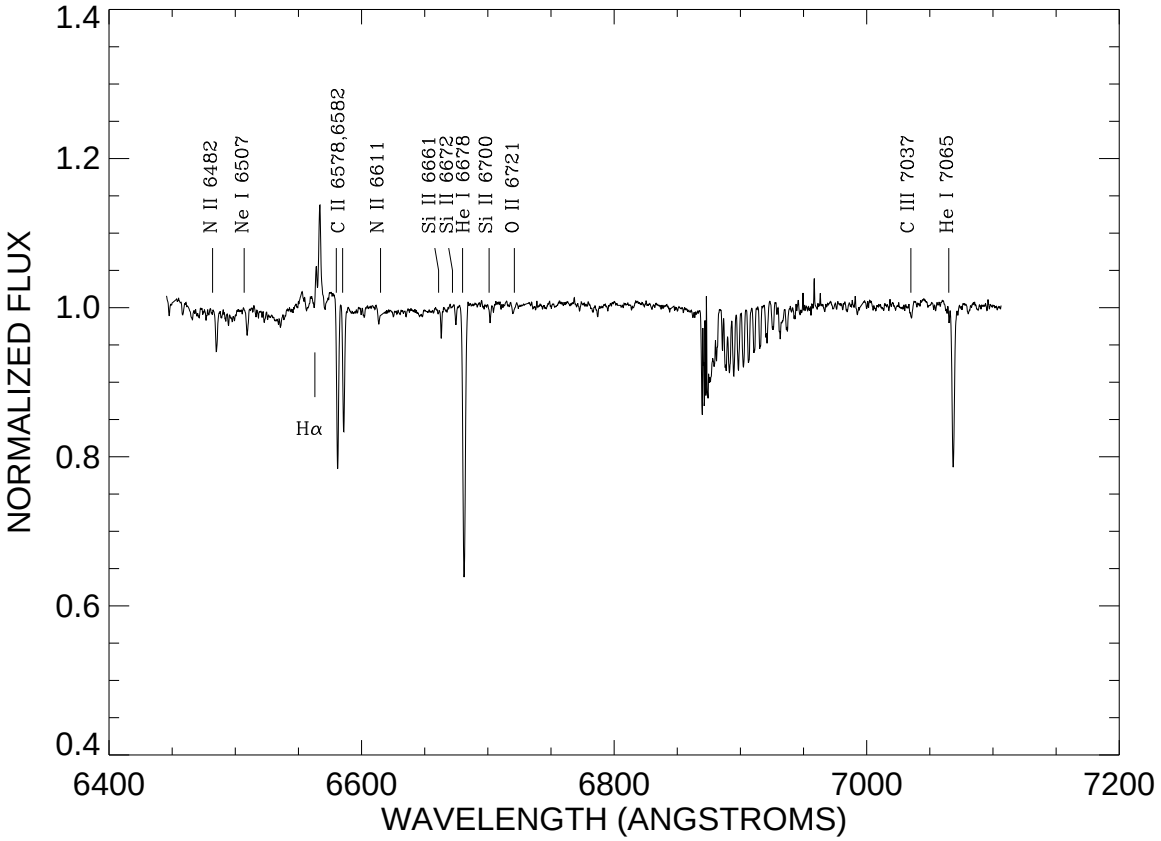

Fig. 6.— Mean spectrum of HD 61827. Features in the 6830−6870 Å region are incompletely removed atmospheric lines.

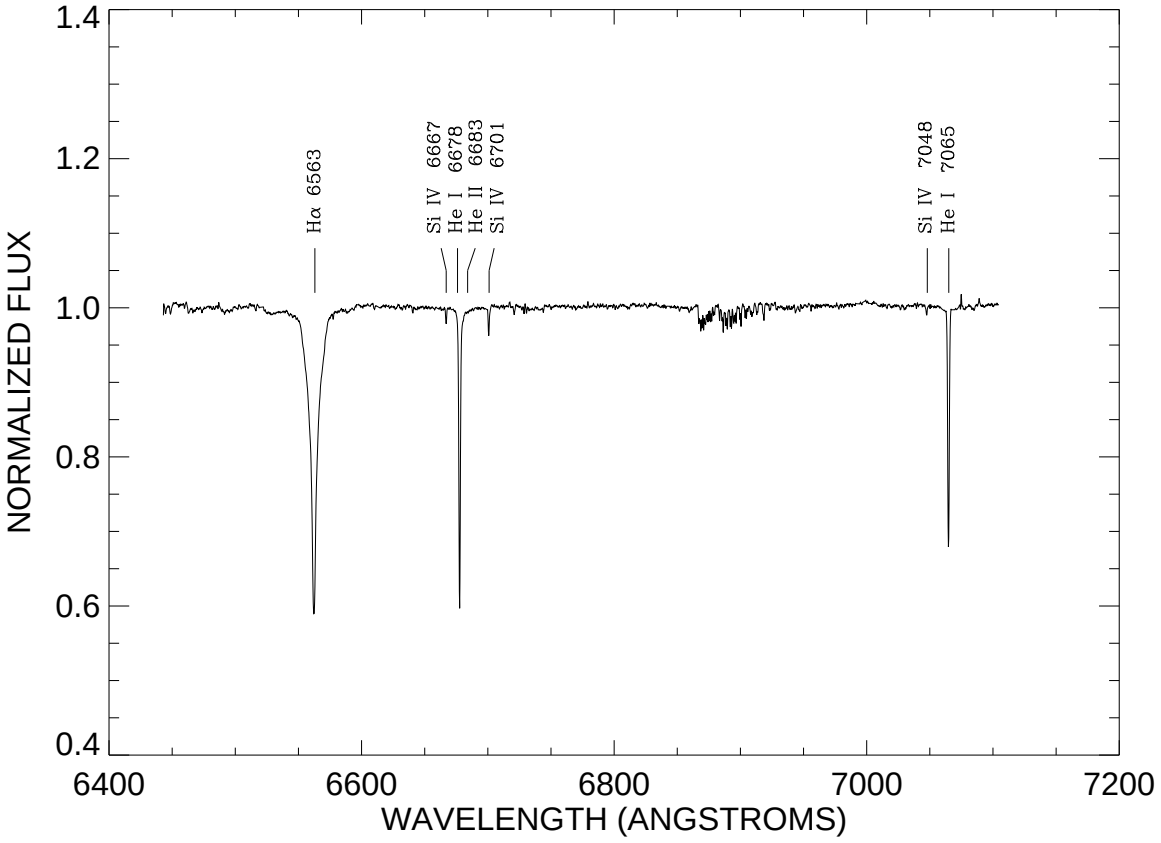

Fig. 7.— Mean spectrum of HD 206183.